Chapter 3

Materials and Methods

Chapter 3 discusses the materials and methods experimental adopted for this investigation. In this chapter the entire work flow chart and its various tests are also presented. It also deals with the chemical and mechanical properties of the base material. A detailed description of the experimental set up, different types of alternating shielding gases, welding procedure and testing methods are also presented.

3. Materials and Method

3.1 Introduction

The objective of the present investigation is to fabricate good quality weld bead and high strength joints of A6061 and A6063 aluminium alloy using MIG Welding Parameters. The experimental work was planned in the following sequence:

(i). Evaluation of base metals properties.

(ii). Fabrication of weld bead using MIG with Welding Parameters

(iii). Fabrication of joints using MIG with Welding Parameters

(iv). Analysing the effect behaviour of Welding Parameters on tensile strength, hardness and macrostructures.

(v). Characterizing the weld region by Optical Microscopy (OM), Scanning Electron Microscopy (SEM), Micro-hardness and X-ray Diffraction (XRD) analysis.

The experimental plan of the present investigation is also illustrated in the form of a flow chart, as shown in Figure 3.1. The detailed experimental procedures involved in each stage of the experimental work are briefed in the following sections.

3.2 Research Methodology

Various concepts about this thesis work were extracted from various academic sources such as ASME welding books, research journal articles related to the objective, previous studies, manual of the company pertaining welding principle, and different websites. Various steps followed during the experimentation can be seen from the flow chart shown in figure 3.1 below.

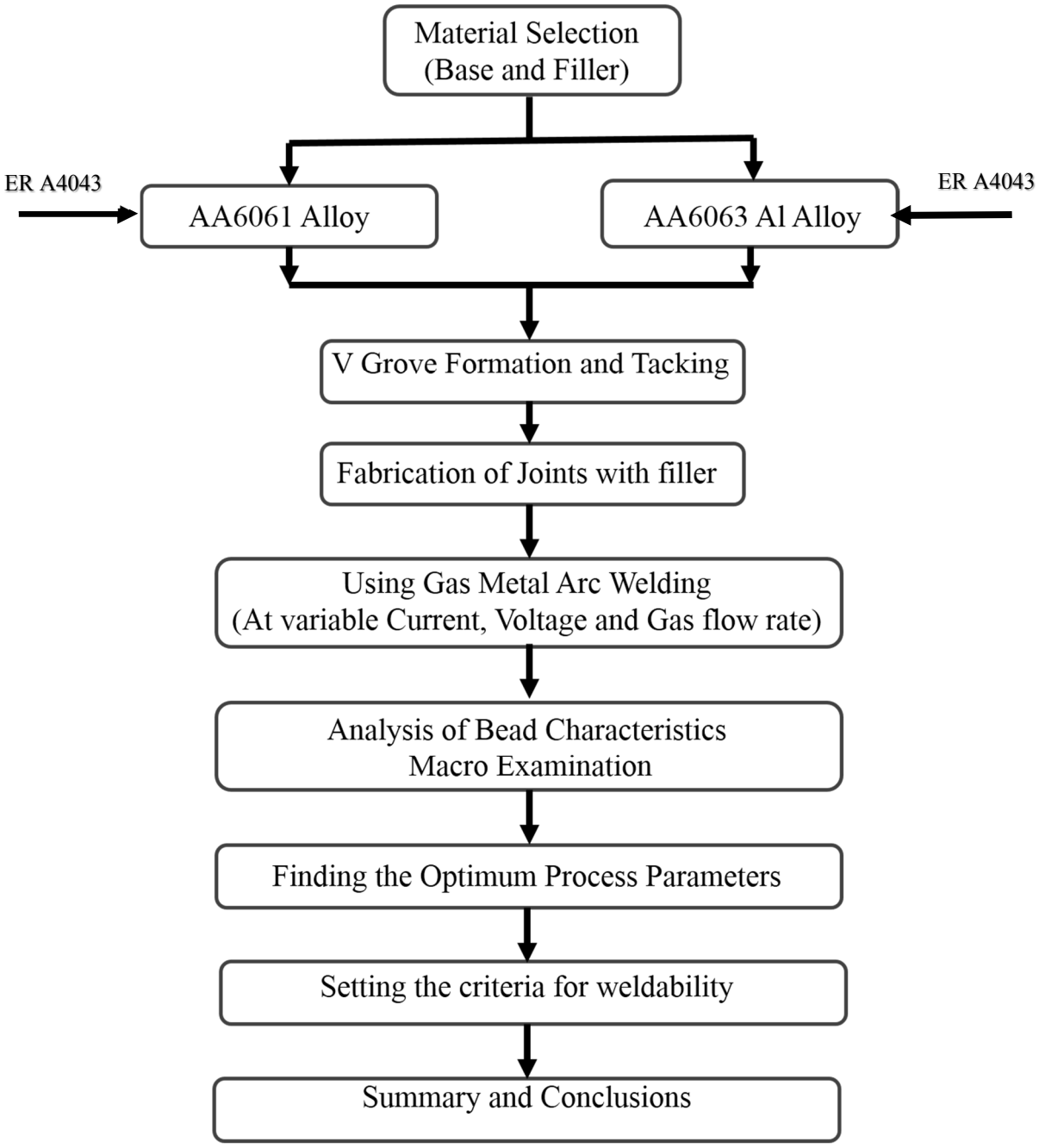

Figure 3.1: Experimental Plan

3.3 Material Selection

3.3.1 Base Materials A6061

The base metals used in this investigation are A6061 aluminium alloy. A6061 aluminium is alloyed with 1.0% magnesium and 0.60% silicon. It has good formability, weldability and corrosion resistance. This material is used in rail coaches body, truck

frames, shipbuilding, bridges, military bridges, aircraft fittings, camera lens mounts, couplings, marine fittings and hardware, electrical fittings and connectors, hinge pins, magneto parts, brake pistons, hydraulic pistons, appliance fittings, valves and valve parts, bike frames etc.

3.3.2 Base Materials A6063

The base metals used in this investigation are A6063 aluminium alloy. A6063 aluminium is alloyed with0.70% magnesium and 0.20% silicon. It has good formability, weldability and corrosion resistance. A6063 often referred to as the “architectural alloy”, is known for providing superior finish characteristics and is often the most useful alloy for anodizing applications.

3.3.3 Filler Material

The filler metal was chosen based on its compatibility with the parent metals. In this study, the filler wire, namely ER4043 was selected as their chemical compositions were matching well with the base metals. ER4043 is a 5% silicon aluminium alloy designed to weld many similar and dissimilar cast and wrought aluminium parts such as the 6XXX base metals and cast alloys. Silicon with this alloy gives improved wetting action yielding a less crack sensitive, bright weld bead. The silicon additions result in improved fluidity (wetting action) to make the alloy a preferred choice by welders. The alloy is less sensitive to weld cracking and produces brighter, almost smut free welds. This alloy is excellent for types A6061, A6063, A4043, A5052, A355, A356 and others. A4043 can be found in many typical welding applications, such as bicycles, trucks and automotive parts and equipment. A 1.6 mm diameter filler wire spool was used during this investigation.

3.3.4 Procured Items

A6061-T6 aluminium alloy and A6063-T6 aluminium alloy from Bharat Aluminium Company Ltd., in plate form having a thickness of 5 mm and filler Metal A4043 from ESAB India, were procured.

3.4 Evaluation of Base Metal Properties

The chemical composition of the base metal was obtained using spark spectroscopy. Sparks were ignited at various locations of the base metal sample, and their spectrum was analyzed for the estimation of alloying elements. The chemical composition (in weight percent) of the base metals is presented in Table 3.1.

Table 3.1: Chemical composition (Wt. %) of A6061, A6063 and ER4043 filler material aluminium alloy

Material	Mg	Si	Fe	Cu	Cr	Mn	Zn	Ti	Al
A6061	1.0	0.60	0.70	0.23	0.01	0.8	0.28	0.15	Balance
A6063	0.7	0.2	0.23	0.1	0.1	0.1	0.1	0.1	Balance
ER4043	0.05	5.5	0.6	0.3	0.1	0.05	0.1	0.1	Balance

Tensile specimens were prepared through milling operation, as shown in Figure 3.2, to obtain the base metal tensile properties. During tensile testing of base metal, ASTM E8M-04 guidelines were followed. The calculated percentage elongation has been tabulated in Table 3.2. Optical micrograph and SEM images

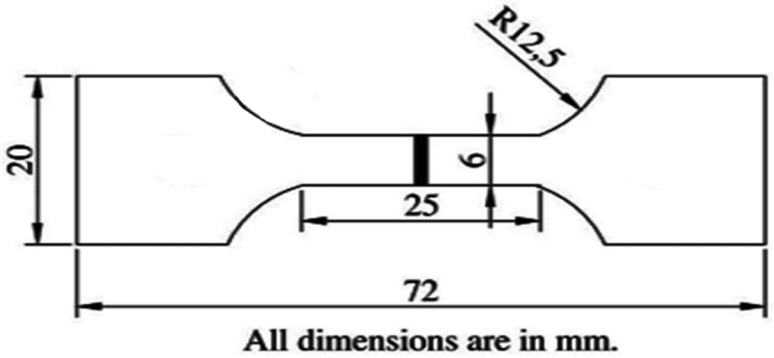

Figure 3.2: Dimensions of the tensile test specimen (ASTM E8)

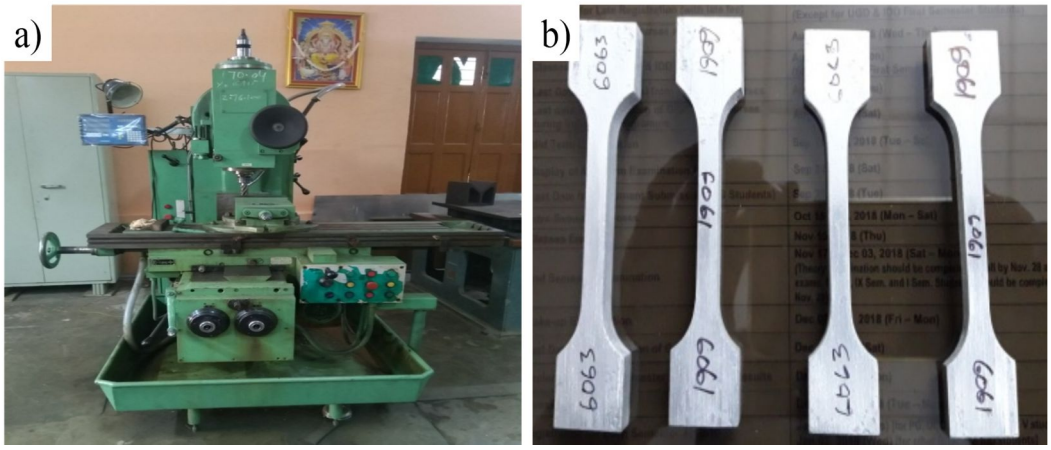

Figure 3.3: (a) Vertical Milling and (b) Tensile specimen of base metals

Table 3.2: Mechanical properties of A6061and A6063 aluminium alloy

Material	Tensile Strength (MPa)	Yield strength (MPa)	Elongation (%)	Hardness (Hv)
A6061	311±7	276±7.5	15±0.6	105±3
A6063	241±8	214±7	11±0	83±3

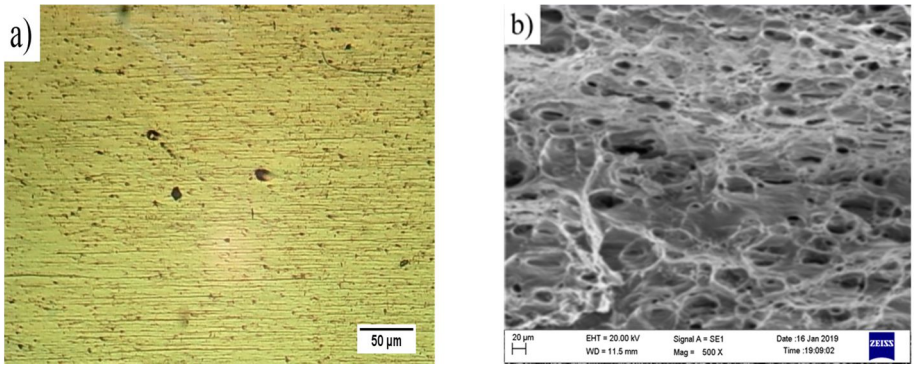

Figure 3.4: Base metal A6061 a) Optical micrograph b) SEM Fractograph

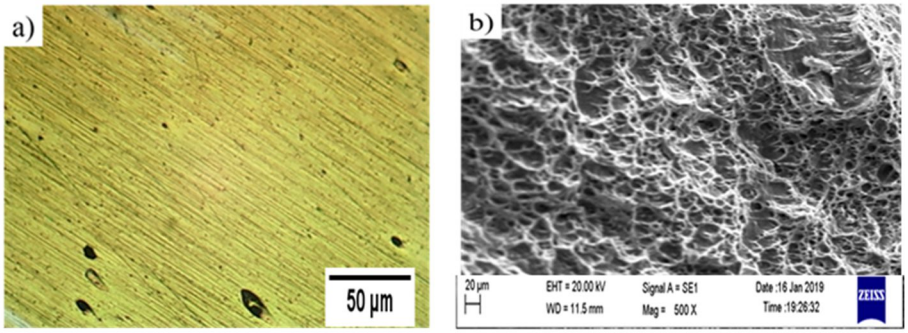

Figure 3.5: Base metal A6063 a) Optical micrograph b) SEM Fractograph

3.5 Experimental Setup

3.5.1 MIG Welding

Experimentation was carried out on 5 mm thick Plates of A6061, and A6063 aluminium alloys were end milled to the required dimensions of 200mmX100mm with an angle of 45^0 in one end only. The included angle of 90^0 for single "V" groove butt joint configuration used was used to facilitate the analysis of welding at different values of chosen parameters. The initial joint configuration with a fixed root gap of 1.4 mm was obtained by securing the plates by tack welds in the roll direction with the help of spacers of 1.4 mm by MIG welding. The tacked plates were thoroughly cleaned to remove the oxide layer using a wire brush followed by acetone before welding and clamped using four C clamps. A schematic diagram of the setup can be seen in figure 3.6, which consists of a welding machine (MIG) and gas cylinders. The 6xxx series Al-Si-Mg alloys possess medium strength and good corrosion resistance. Alloys 6061 and 6063 are widely used for welded structures. The selection of filler wire is least cracking tendency and salt water corrosion resistance. Almost smut free welds can be obtained. [American Welding Society, 2004.]

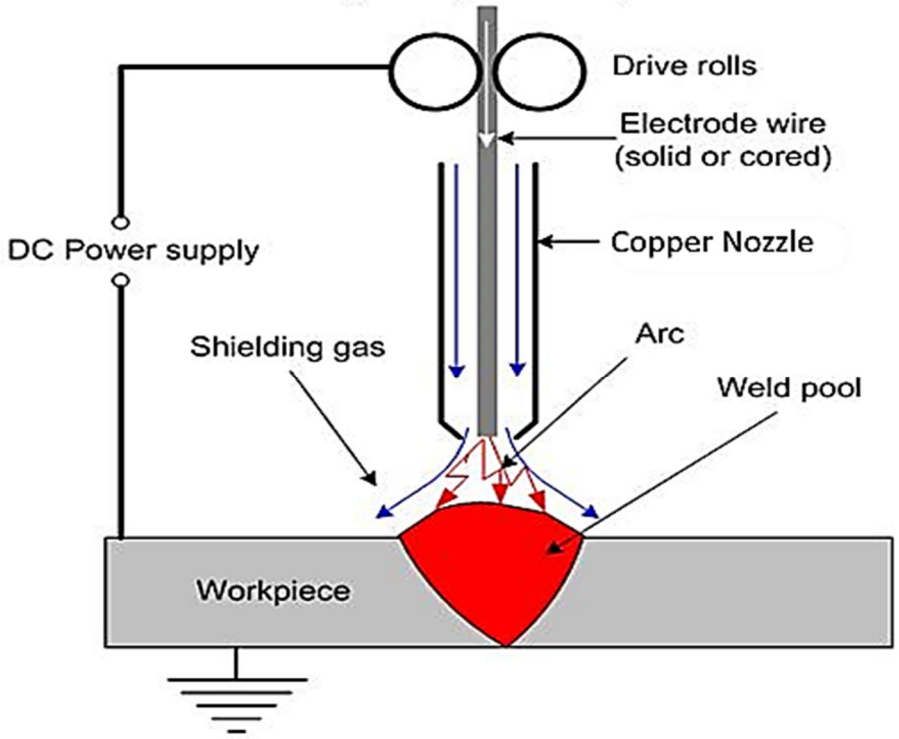

Figure 3.6: Schematic diagram of MIG welding process

The automatic MIG welding machine (ESAB RC-AUTO-K400) was used for welding the workpieces at various welding currents, Voltage and gas flow rate in Direct Current Electrode Positive (DCEP) mode. DCEP mode leads to a larger amount of heat generation (approx. two-third of the total heat generated) at the filler metal end. The welding direction was a backward hand with a torch angle of 10^0 to the normal direction, as the torch angle dictates the shielding gas flow direction and proper shielding of the weld pool. High purity commercial-grade argon gas (99.99%) was used as the shielding gas because of the formation of an oxide layer which makes a protective layer causing defects in weld joint due to its high melting point. Initially, pilot runs were carried out for various current and voltage combinations to find out the optimum process parameters like Current (I), Voltage (V), Gas flow rate (f), Root gap (S) etc. The actual setup can be seen in Figure 3.6.

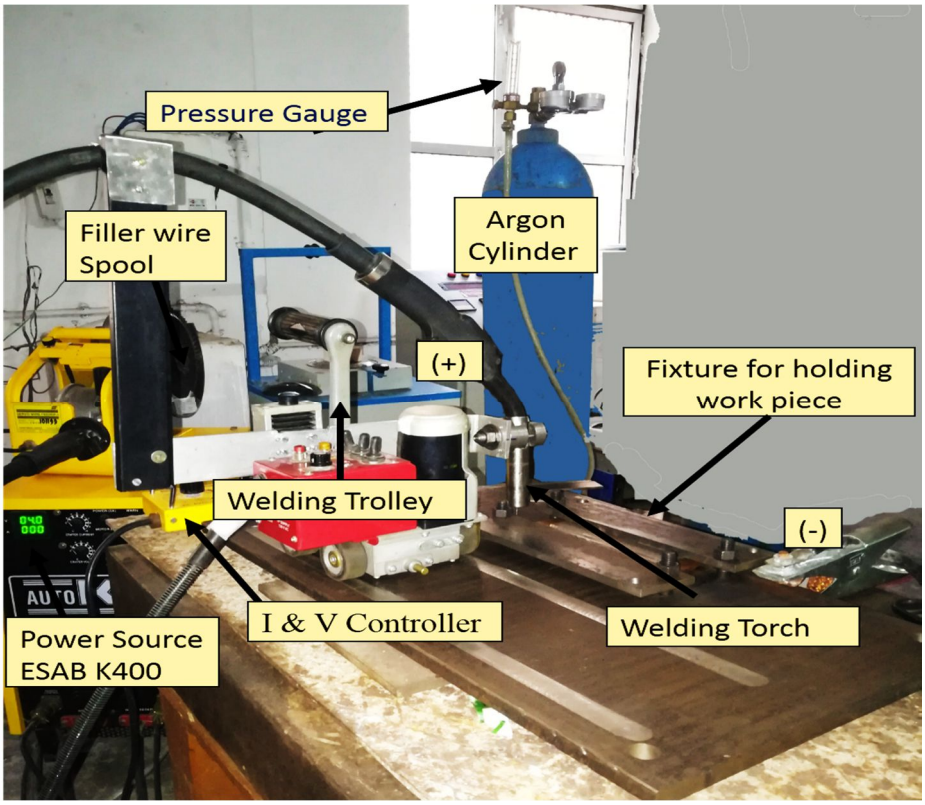

Figure 3.7: Actual Setup of MIG used for experimentation

Argon gas cylinders are equipped with a flow meter to monitor the gas flow rate of the cylinder. Nozzle standoff distance was kept fixed at 12mm. Welding was performed using Ø1.6 mm diameter filler wire of Al4043 grade at aforesaid welding parameters. Al4043 filler metal is an all-position 5% Si alloy preferably used to join heat treatable similar alloys. It improves puddle fluidity, producing a smooth bead profile and low crack sensitivity on the magnesium-silicon aluminium alloy. The Chemical composition of base metal and filler metal, examine by optical emission spectrometer (Foundry Master) and are listed in Table 3.1. The joints without surficial defects were investigated through metallography, hardness and tensile tests.

3.5.2 Supply of Shielding Gas

The technology of the shielding gas supply affects every aspect of the quality of arc welding. The technology's benefits are driven primarily by the dynamic action caused to the molten pool of welds. The supply of shielding gas produces three independent

phenomena, (a) Arc pressure variation, (b) Variation in weld pool fluidity and (c) Arc pressure peaking, each complementing the other two to create the stir in the weld pool. When Ar passes, the pool temperature is low, and fluidity is low, whereas when He flows, the pool temperature is high, and its fluidity is high. As the shield gas alternates, the pool experiences changes in temperature and fluidity. The net result is a stirring motion on the weld pool. The conventional use of shield gas or premixed shield gases produces a constant arc pressure and constant pool fluidity over time.

3.5.3 Fabrication of Beads and Joints

The rolled plates of A6061and A6063 aluminium alloy of 5 mm thickness were machined to the specific dimensions (100mmX 200mm). Before welding, the base material was cleaned carefully to remove contamination like rust, dust, oil, moisture etc. So, to avoid welding defects due to contamination of the base metal. During welding, the plate was rigidly fixed by suitable clamps. Single-pass, the autogenously welding procedure was applied to perform bead on plate experiments on plates of A6061and A6063 for 200 mm length. In order to obtain a variety of heat inputs, welding Current, Voltage and gas flow rate was varied at constant welding speed. Different levels of Current, Voltage and Gas Flow Rate used for welding at cons taint weld speed has been shown in Table 3.3 shown below.

Table 3.3: MIG welding parameters for experimentation

Parameters	**Level 1**	**Level 2**	**Level 3**
Current (Amp.)	140	160	180
Voltage(Volts)	15	18	21
Gas Flow Rate(LPM)	10	14	18
Welding Speed (mm/sec)	2.5	2.5	2.5

Levels of parameters have been used for making full penetration welds in accordance with literature and minimizes the number of experiments which ultimately reduces the overall cost of experimentation.

The bead on plate experiments was performed on the base plate using a stringer bead method. In order to obtain a good quality weld bead, the process parameters of welding were carefully controlled. It was ensured that the weld beads were free from defects like surface porosity and blowholes. The rolled plates of A6061 and A6063 aluminium alloy were machined by a milling machine to the required dimensions (100 mm×200 mm). Single 'V' butt joint configuration, as shown in Figure 3.8, was prepared to fabricate MIG welded joints. The used groove design is as per ASTM standard and are used and available in various literature (Y. Balram et al.2019).

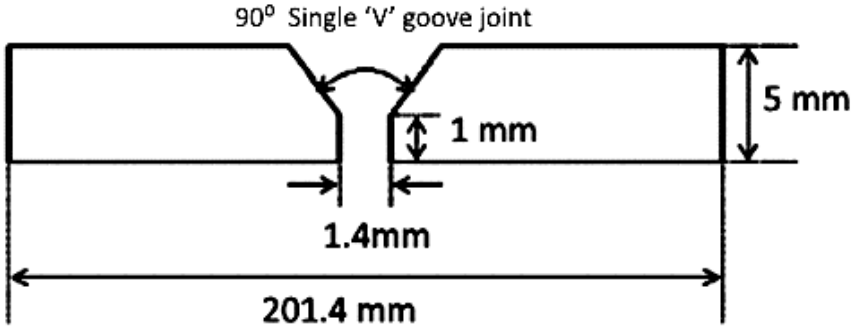

Figure 3.8: Joint configuration for MIG welding

The initial joint configuration was obtained by securing the plates in position using tack welding for MIG welds. The direction of welding was normal to the rolling direction. The clamping technique was applied using appropriate types of clamps in order to avoid joint distortion. All necessary care was taken to prevent joint distortion. Single-pass.

An autogenous welding procedure was applied to fabricate the joints using MIG welding. High purity (99.99%) argon gas were used as shielding gas with a flow rate of 10-18 L/min. ER4043 grade filler wire of 1.6 mm diameter was used for MIG welding. Welded samples for both the alloys have been shown in figure 3.9.

Figure 3.9: The Welded plates of a) A6061and b) A6063

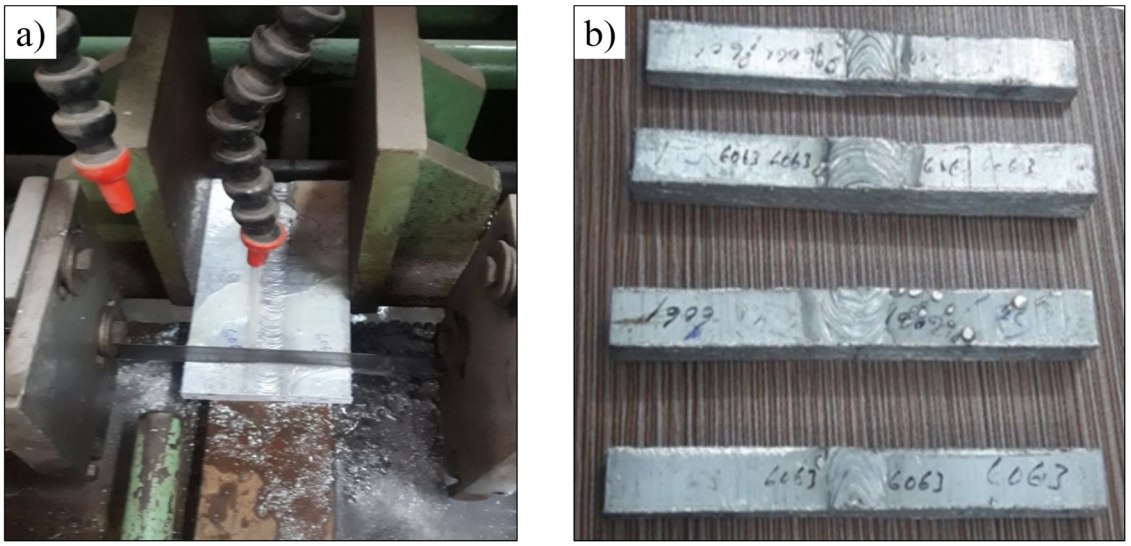

Figure 3.10: (a) Band saw and (b) fabricated samples for microstructure and hardness test

Grinding and Belt lancing machine was used to fabricate the specimens from the welded joint for microstructure, tensile test and hardness from locations shown in figure 3.10

3.6 Characterization

Specimens for various characterizations were machined from Welded joints. The strategies followed for samples extraction for various characterizations is shown schematically in Figure 3.11.

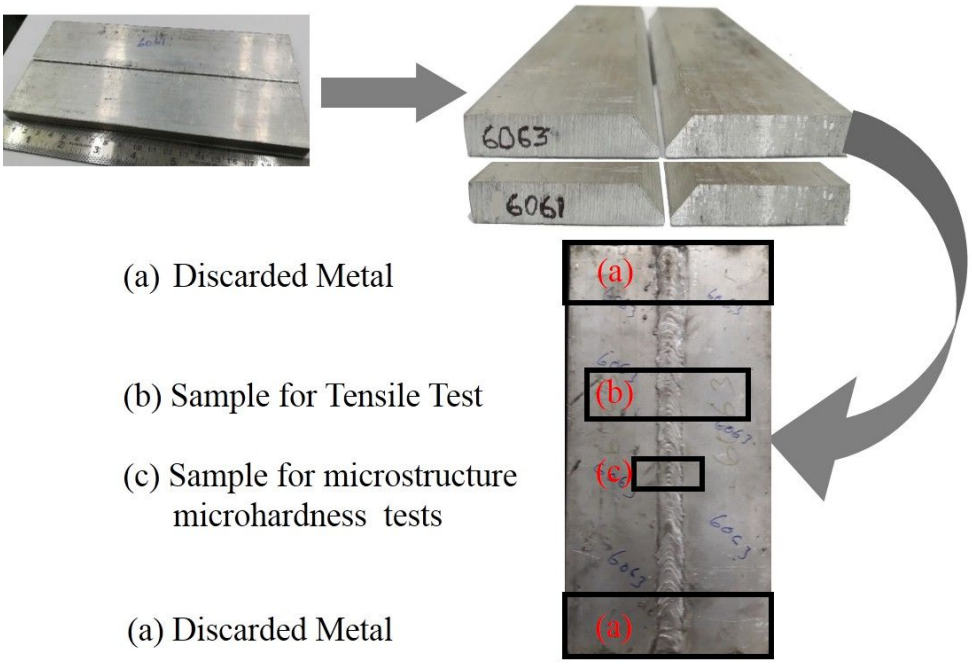

Figure 3.11: Steps followed during fabrication and sample extraction for analysis

The microstructural features were observed by optical microscopy and scanning electron microscopy, whereas the compositional analysis was performed through X-ray diffraction. The various tests performed to assess the performance of the composites were macrostructure Micro-hardness and tensile test for both welded alloys.

3.6.1 Evaluation of Bead Profile Characteristics

Transverse sections of each weld bead were obtained using a high-speed SiC abrasive cutter after discarding 50 mm of the bead length from either end. The schematic diagram shown in Fig 3.14 illustrates the preparation of specimens for carrying out the macro tests. All the test specimens were ground and polished. Polishing was carried out as per the metallurgical practice on a set of five emery papers changing successively the direction of polishing by 90° when moved from rougher to finer emery. The polished samples were etched with Keller's solution to get a clear view of the various sections of the weldment. All the samples were microscopically scanned at 10X magnification using

a stereo microscope to visualize the bead geometry, as shown in Figure 4.15. The weld bead dimensions such as bead penetration depth, bead penetration area, bead width, bead reinforcement area, reinforcement height and wetting angle were measured from magnified images of the weld bead. The magnified images were imported into AutoCAD. Imported images were scaled appropriately to match the known thickness of 5 mm. From these scaled images, bead geometry dimensions were measured using AutoCAD. The size of the fusion zone on the top surface of the base plate is estimated as the weld bead width. The penetration is measured from the top surface of the base plate.

Figure 3.12: Stereomicroscope

3.6.2 Macro and Microstructural Analysis

For microstructural examination, specimens were prepared according to metallographic standard, i.e. grinding (SiC emery papers) using emery paper of grit sizes 600, 800, 1200, 1500 and 2500 from lower to the higher grade. Followed by mechanical polishing with 0.2~0.5 μm sized diamond paste along with aerosol lubricant to have maximum conformity. The chemical etchant used was Kellers' Reagent (3 ml HF in 100 ml of water) for 20 sec to visualize the grain boundaries. The chemically etched samples were observed under an optical microscope (Leitz Metallux-3). Optical Microscopy (OM) was used to capture the macro and microstructure of the weldments. A qualitative macroscopic inspection of the weld zone was performed by visual inspection of

macroscopic images. The weldment image provided significant information about the fusion zone like the depth of penetration, weld bead width, the number of passes and HAZ width (using microstructure). Macrostructural and microstructural studies of the weldment cross-section was observed using a stereo optical microscope. Specimens were etched with Keller's reagent to reveal the microstructure. These microstructures were used to study the changes that occurred in the grain structure of the weldment due to the effect of heat input. The grain size distribution was analyzed through ImageJ software.

3.6.3 X-Ray Diffraction (XRD)

The samples were extracted from the weld region in the dimension of 10mmX19mm (Max.) to identify the phase constitution near the weld zone of the MIG welded joints. X-ray diffraction study was carried out for compositional analysis by using a diffractometer (Model- MINIFLEX 600 DETEXULTRA, Japan). Cu-Kα radiation of wavelength 1.5402 A° with Ni filter was used. 3.12. The analysis was carried out in Theta-Theta (Vertical type), D/Max with the copper target under a working voltage of 40 kV and 40 mA working current. A scintillation counter detector was used with a scan range of 3° to 154°(2Ø). The results obtained are evaluated with data from the Joint Committee on Powder Diffraction Standards (JCPDS).

3.6.4 Tensile Test

Tensile Testing Machine: A computerized 100 kN screw-driven Instron™ Universal Testing Machine. According to ASTM E8/8M standard, the transverse tensile specimens were prepared from the weldments with the cutting axis perpendicular to the weld fusion zone. The schematic diagram 3.16 shows the section plan for tensile test and microstructure specimen. Two test trials on the weldments were conducted to check the reproducibility of the results. The tensile testing of weldments is more focused on the fusion zone than the base metal as the weldment is heterogeneous in nature, composed of

the deposited weld metal, the HAZ and the unaffected base metal. Transverse tensile specimens provide joint efficiency in terms of strength. As shown in Figure 3.13, the tensile tests were carried out using FIE make Universal Testing Machine, which has a maximum capacity of 100KN. The specimen was loaded at the rate of 1.5 kN/min as per ASTM specifications so that the tensile specimen undergoes uniform deformation. The specimen finally failed after necking, and the load versus displacement was recorded.

Figure 3.13: Universal Testing Machines (UTM)

3.6.5 Scanning Electron Microscopy (SEM)

The dendritic structure and intermediate phases in the weld bead were analyzed under Scanning Electron Microscopy (SEM). The samples for SEM analysis were also extracted exactly in the same manner as it was taken out for optical microscopy. The dimensions of the specimens were 10mm x 10mm. Specimens were first polished on different grades of emery papers (400~2000 grit size), and then it was mechanically polished with diamond paste. The samples were not chemically etched. The mechanically polished samples were observed on SEM (Serial no. EVO18-20-45, ZEISS EVO 18

RESEARCH, Germany). The fracture behaviour of the samples resulting from tensile testing was also characterized using SEM.

3.6.6 Hardness Test

Microhardness Tester: Model- MINIFLEX 600 DETEX ULTRA, Japan as shown in Figure 3.18, three distinguished regions such as base metal (BM), HAZ and weld metal (WM) were identified. The hardness test specimens were prepared from the welded samples. Waldport group make Vickers hardness testing machine was used to measure the hardness. A standard test load of 0.5 Kg was applied for a dwell period of 10 s. For analysis of hardness, the measurements/ indentations were taken at an interval of 0.5 mm with respect to the centre of the weld bead on the surface along the transverse section of each region. The hardness profiles were generated based on the results, and the hardness trend was carefully assessed to understand the hardness variation across welded joints.

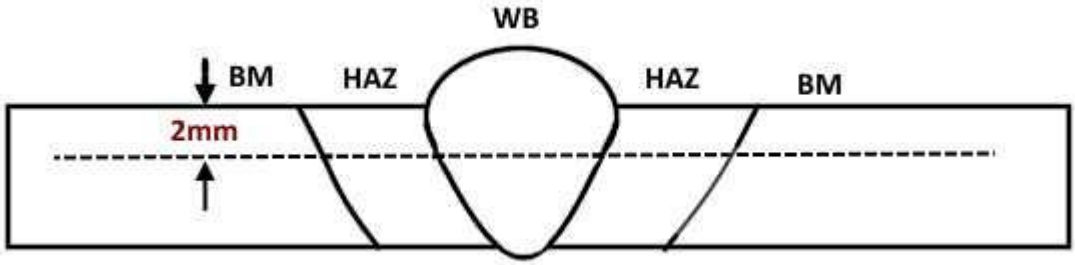

Figure 3.14: Location of hardness measurement across welded joints

3.7 Summary

This chapter dealt with the materials, welding procedures, various welding parameters current, Voltage and gas flow rate and various testing methods used in the present investigation. It also deals with the chemical composition and mechanical properties of the base materials. Moreover, the chapter also describes the welding machine and different welding parameters selected for conducting the experiments. It also explains the various mechanical and metallurgical testing procedures and their corresponding specimen preparations based on various ASTM standards. The results

obtained from the experimental works are presented, analyzed and discussed in the following chapters.